Talanta 79 (2009) 38–45

Contents lists available at ScienceDirect

Talanta

journal homepage: www.elsevier.com/locate/talanta

Amperometric biosensor for hydrogen peroxide based on coimmobilized horseradish peroxidase and methylene green in ormosils matrix with multiwalled carbon nanotubes

A.K. Upadhyay, Tzu-Wei Ting, Shen-Ming Chen*

Department of Chemical Engineering and Biotechnology, National Taipei University of Technology, No. 1, Section 3, Chung-Hsiao East Road, Taipei 106, Taiwan, ROC

ARTICLE INFO

Article history:
Received 31 December 2008
Received in revised form 1 March 2009
Accepted 2 March 2009
Available online 14 March 2009

Keywords:
Multiwalled carbon nanotubes
Methylene green
Ormosils
Horseradish peroxidase
Hydrogen peroxide

ABSTRACT

A novel amperometric biosensor for the analytical determination of hydrogen peroxide was developed. The fabrication of the biosensor was based on the coimmobilization of horseradish peroxidase (HRP), methylene green (MG) and multiwalled carbon nanotubes within ormosils; 3-aminopropyltrimethoxysilane (APTMOS), 2-(3,4-epoxycyclohexyl)ethyltrimethoxysilane (ETMOS) and phenyltrimethoxysilane (PHTMOS). APTMOS determined the hydrophilicity/hydrophobicity of the ormosils and PHTMOS and ETMOS increased the physical and mechanical strength of the ormosil matrix. The ormosil modified electrodes were characterized with SEM, UV–vis spectroscopy and electrochemical methods. Cyclic voltammetry and amperometric measurements demonstrated the MG coimmobilized with HRP in this way, displayed good stability and could efficiently shuttle electrons between immobilized enzyme and electrode, and MWCNTs facilitated the electrocatalytic reduction of H_2O_2 at reduced over potential. The Micheaelis constant of the immobilized HRP was 1.8 mM, indicating a high affinity of the HRP to H_2O_2 without loss of enzymatic activity in ormosil matrix. The prepared biosensor had a fast response of H_2O_2, less than 10 s, and excellent linear range of concentration from 5×10^{-7} to 2×10^{-5} M with the detection limit of 0.5 μM (S/N = 3) under the optimum conditions. At the same time, the influence of solution pH, effect of enzyme amount, steady-state applied potential and temperature on the biosensor were investigated. The enzyme electrode retained about 90% of its initial activity after 30 days of storage in a dry state at 4 °C. The preparation of the developed biosensor was convenient and showed high sensitivity with good stability.

1. Introduction

The rapid, accurate, reliable and simple analytical determination of hydrogen peroxide is of great importance in clinical, industrial, pharmaceutical, food industry and environmental [1–5] analyses. Conventional hydrogen peroxide determination methods, such as fluorimetry [6,7], titrimetry [8], spectrometry [9] and chemiluminescence [10,11] are generally time consuming and cumbrous for operation. Now the electrochemical method displays better prospects due to its advantages of easy preparation, fast detection, low consumption of reagents and high selectivity and sensitivity [12]. Nowadays, horseradish peroxidase (HRP) has been widely used for the fabrication of ormosil based amperometric biosensors to the detection of H_2O_2 due to its high purity, sensitivity, low cost and easy availability [13–15].

Carbon nanotubes (CNTs) have attracted considerable study since their discovery [16]. Due to their high electrical conductivity, strong absorptive properties, good mechanical strength and excellent biocompatibility, currently biomolecules have been successfully integrated with MWCNTs. The integration of biomolecules with MWCNTs enables the use of such hybrid system as electrochemical biosensors (enzymes electrodes, DNA sensors or immune sensors) [17–20]. The MWCNT-based biosensors offer substantially greater signals especially at low potential, reflecting the electrocatalytic activity of MWCNTs. Such low-potential operation of MWCNT-based biosensor results in a wide linear range and fast response time. Several number of amperometric peroxide biosensors have been fabricated based on NAD^+ and SWNT modified electrode [21], poly(TB)/HRP/MWCNT/chitosan modified electrode [22], MWCNT/polysulfone modified electrode [23], MWCNT/BSA/HRP/ferrocene modified electrode [24], MWCNT/HRP/MB modified electrode [25], silica-hydroxyapatite/HRP nanocomposite modified electrodes [26], TiO_2/DNA/thionin nanocomposite modified electrode [27], Au-modified TiO_2 nanotube arrays/HRP modified electrode [28] and

* Corresponding author.
E-mail address: SMChen78@ms15.hinet.net (S.-M. Chen).

0039-9140/$ – see front matter © 2009 Elsevier B.V. All rights reserved.
doi:10.1016/j.talanta.2009.03.010

CNT/ABTS/HRP based modified electrode [29]. Xie and co-workers developed third-generation biosensor for H_2O_2 on the basis of the immobilization of horseradish peroxidase (HRP) in a nanocomposite film of tetrathiafulvalene–tetracyanoquinodimethane (TTF–TCNQ)/multiwalled carbon nanotubes (MWCNTs) modified gold electrode [30]. A series of water soluble organic dyes have been used as mediators in solution, due to their excellent mediating ability and low cost. But in solution, dye molecules will not only pollute the reference electrode and counter electrode, also decrease the analytical sensing ability of sensor, due to deposition it on the electrode surface. Therefore, it would be preference to immobilize the dye on the electrode surface. To overcome this critical issue, we used organically modified sol–gel glasses (ormosils) to encapsulate the dyes/biomolecules. The dye strongly interacts with the silanol groups of the porous surface and remains in a more restricted environment at the ormosils than it is at the gel–glass cage. This observation indicates the ormosils would be a suitable host for dyes. Several redox dyes such as, methylene blue [31], methylene green (MG) [32], meldola blue [33] and Celestine blue [34] can be used as electron transfer mediators when immobilized on the electrode surfaces. The leaching of biomolecules from the electrode surface during electrochemical characterization is a crucial problem in the fabrication of electrochemical biosensor. Ormosils are the unique matrices to encapsulate the biomolecules [35–38], due to their inert chemical nature, high mechanical strength, excellent optical properties, strong adhesion properties to its surface support and ease of modification. The incorporation of organic moieties increases the crosslinking in the matrix and provides improved electron transportation. The ormosil modified electrodes possesses a large potential window, low and almost constant background current over a large potential window, and fast kinetics for a large number of electrochemical mediators. The intersection of ormosil with MWCNT will be a valuable asset in the field of development of biosensor because the ormosils are the appropriate matrices for the encapsulation of biomolecules (enzyme, protein, DNA, etc.) and MWCNTs provide better conductivity than graphitic carbon to its unique physical and chemical properties.

In this article we prepared a highly sensitive and selective H_2O_2 biosensor using three types of ormosils; 2-(3,4-epoxycyclohexyl) ethyltrimethoxysilane (ETMOS) phenyltrimethoxysilane (PHTMOS), and 3-aminopropyltrimethoxysilane (APTMOS). Methylene green (as mediator) and HRP were coimmobilized within the ormosils matrix with MWCNTs. The presence of organic functional moieties in the ormosil, provide strong cage to the encapsulating small molecular size enzymes to remove the leaching problem. The widely present amino groups in ormosils provide a hydrophilic microenvironment that is compatible with the biomolecules [39] and increase the stability of the biosensor. Cyclic voltammetric and amperometric measurements were carried out to demonstrate the feasibility of MG as an electron shuttle between the immobilized peroxidase and a glassy carbon electrode. MWCNTs incorporated within ormosils facilitating the electron-transfer reaction between the enzyme and the electrode. The resulting biosensor exhibited high sensitivity and much better stability than the developed biosensor based on the coimmobilization of horseradish peroxidase and methylene blue on a CNT modified electrode [25], and methylene blue/SiO_2 nanocomposite modified electrode [40].

2. Experimental

2.1. Reagents and materials

Peroxidase from horseradish (POD, EC 1.11.1.7 type VI) was obtained from Sigma; methylene green was purchased from Fluka. phenyltrimethoxysilane, 3-aminopropyltrimethoxysilane, 2-(3,4-epoxycyclohexyl)ethyltrimethoxysilane, *N,N*-dimethylformamide (DMF) and multiwalled carbon nanotubes (10–15 nm diameter) were purchased from Aldrich Chemical Co. Hydrogen peroxide (30%, w/v solution) was purchased from Wako Pure Industrial Co., Japan. The concentrations of more diluted hydrogen peroxide solutions were determined by titration with cerium(IV) to a ferroin end point. Phosphate buffer solutions (PBS) of various pH were prepared with 0.1 M KH_2PO_4 and 0.1 M Na_2HPO_4 with supporting electrolyte 0.1 M KCl. All other chemicals employed were of analytical grade. All the solutions were prepared with doubly distilled water.

2.2. Apparatus

The electrochemical measurements were performed with a computer controlled CHI750A (TX, USA) electrochemical system. Cyclic voltammetry and amperometric measurements were done with a three electrode system comprising the MG/HRP/GCE and MWCNTs/MG/HRP/GCE as a working electrode, an Ag/AgCl reference electrode and platinum wire as counter electrode. All electrochemical measurements were carried out in 5 ml (0.1 M, pH 7.2) phosphate buffer solution (PBS). All experimental solutions were thoroughly deoxygenated by bubbling nitrogen through the solution for at least 15 min. Hitachi scientific instruments (Japan) Model S-3000H scanning electron microscope and Hitachi scientific instruments (Japan) Model U-3300 UV–vis spectrophotometer were used for surface image and UV–vis spectra measurements, respectively.

2.3. Fabrication of H_2O_2 biosensor

A glassy carbon electrode (GCE, 3 mm in diameter) was polished with 1.0, 0.3 and 0.05 μm Al_2O_3 slurry successively followed by rinsing thoroughly with double distilled water until a mirror-like surface was obtained. Then it was washed ultrasonically in 1:1 nitric acid, absolute ethanol and double distilled water, each for 5 min, and allowed to dry at room temperature. Two types of ormosils modified electrodes (OME) were fabricated based on the composition given in Table 1.

(A) MWCNTs/MG/HRP/GCE: 75 μl of 3-aminopropyltrimethoxysilane, 10 μl (1 mM) of methylene green and 225 μl of doubly distilled water were mixed in a cell with constant stirring, followed by the addition of 50 μl (1 mg/ml) of horseradish peroxidase (HRP) and 30 μl (1 mg/ml in DMF) of MWCNTs in same solution and stirred for 5 min to get homogeneous solution. After that 2-(3,4-epoxycyclohexyl)ethyltrimethoxysilane,

Table 1
Composition of Ormosils modified electrodes.

OME	APTMOS (μl)	ETMOS (μl)	PHTMOS (μl)	MG (1 mM) (μl)	HRP 1 mg/ml (μl)	DD water (μl)	MWCNTs (1 mg/ml in DMF) (μl)	HCl (μl)
1	75	10	5	10	50	225	–	10
2	75	10	5	10	50	225	30	10

OME: ormosils modified electrode, APTMOS: 3-aminopropyltrimethoxysilane; ETMOS: 2-(3,4-epoxycyclohexyl)ethyltrimethoxysilane; PHTMOS: phenyltrimethoxysilane; MG: methylene green; HRP: horseradish peroxidase; MWCNTs: multiwalled carbon nanotubes.

phenyltrimethoxysilane and 0.1N, 10 μl HCl were mixed and stirred for 10 min to allow to completion of hydrolysis. The prepared ormosil film was smooth and crackfree.1.4 μg of HRP enzyme was deposited on the electrode surface.

(B) MG/HRP/GCE: This ormosils modified electrode was prepared as the same procedure mentioned for ormosils modified electrode A and differ only the absence of MWCNTs. 10 μl of the prepared homogeneous solution was added over the glassy carbon electrode followed by multiwalled carbon nanotubes modified ormosils formation for 6–7 h at room temperature. The OMEs were washed in phosphate buffer (0.1 M, pH 7.2) followed by incubation of electrodes for 4 h in same buffer.

3. Result and discussion

3.1. Physical characterization

3.1.1. SEM and AFM of ormosil modified composite

The physical morphology also affects the response of the enzyme electrode. Thus, the study of surface morphology of the ormosils modified matrix is an important factor affecting its analytical performance. Fig. 1a and b shows the SEM of different surfaces. Fig. 1a is the image of ormosils immobilized with spherical particles of HRP. The immobilized HRP ormosils electrode surface was smooth and indicates that the enzyme was successfully incorporated within ormosils matrix. Fig. 1b displays the SEM image of MWCNTs and HRP within ormosils matrix. It was shown that the MWCNTs (diameter in the range of 30–50 nm) was spread around and equally distributed in the ormosil matrix. The surface of the MWCNTs became rough due to presence of enzyme. It suggested that HRP enzymes disperse along the side walls of MWCNTs in the ormosils film. Therefore, the uniform and open nanostructure provided a significant increase of effective surface for HRP enzyme loading and a good preparation reproducibility of the biosensor.

Typical AFM image (tapping mode) of the MWCNTs/MG/HRP in ormosil composite was shown in Fig. 1c. The thickness of MWCNTs/MG/HRP/Ormosils layer was about 100–108 nm (estimated from the AFM image) and showed an island-like structure. The height difference between the bright region and the dark ground was about 20 nm. The AFM measurement of HRP immobilized in MWCNTs/MG/Ormosil indicated that the deposited enzyme formed a uniform layer with globular shape. The bright regions indicated the presence of MWCNTs in the ormosil film. These features would help in retaining of dopants for long time and improving the electrochemical behavior of the film.

3.1.2. UV–visible spectra of ormosil modified composite

Fig. 2 shows the UV–vis spectra of the MG in water and MG incorporated with HRP in ormosils from 300 to 800 nm. The UV–vis spectrum for the MG head peaks at 664 and 610 nm (Fig. 2, curve a). In the case of MG incorporated within ormosils composites (Fig. 2, curve b), the absorption peaks at 664 nm disappeared, due to interaction between MG and SiO_2 present in ormosils, whereas the peak at around 610 nm shifted slightly towards lower wavelength at 590 nm (blue shift, by about 20 nm) and showed the dimeric form of the dye [41]. The absorption observed at 403 nm corresponds to the HRP heme group absorption and revealed that the HRP was successfully immobilized within the matrix and retained enzymatic properties in ormosil film.

3.2. Electrochemical studies of MWCNTs/MG/HRP/GCE

Fig. 3 displays the typical cyclic voltammograms of MG/HRP/GCE and MWCNTs/MG/HRP/GCE incorporated within ormosils, over a potential range from 0.0 to −0.4 V in 0.1 M PBS (pH 7.2) at different

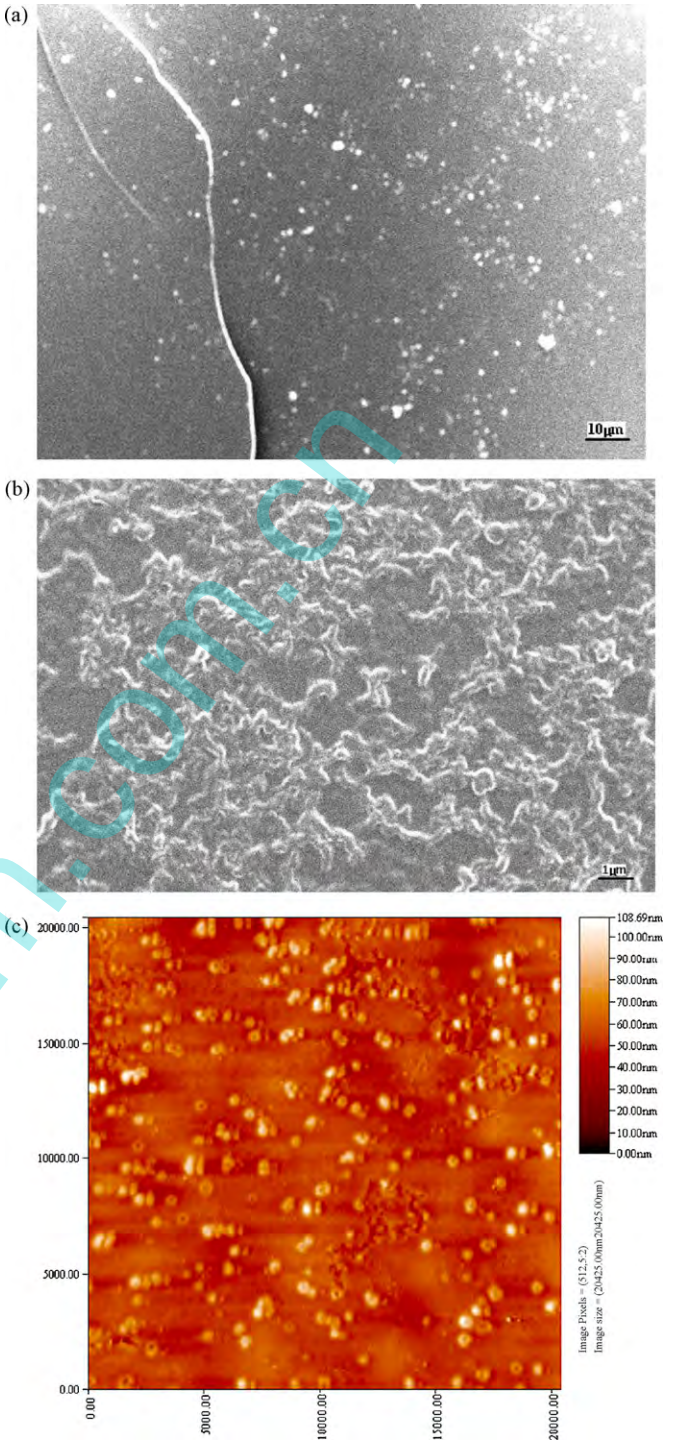

Fig. 1. Typical SEM of ormosils/HRP in the absence of MWNTs (a) presence of MWCNTs (b) composite film on the surface of ITO glass and (c) AFM image of the MWCNTs/MG/HRP composite film coated on ITO glass.

scan rates. Fig. 3b illustrated the remarkable significance of MWCNTs in the electrochemical behavior of modified electrode. The modified electrode with MWCNTs shows a well defined reversible voltammogram corresponding to the redox reaction of MG. Multiwalled carbon nanotubes not only increase the peak current, also improved the redox nature of methylene green incorporated within ormosils because the MWCNTs increase the effective surface area of modified electrode. The peak separation (ΔE_p) was typically small (~35 mV) and the ratio of anodic and cathodic

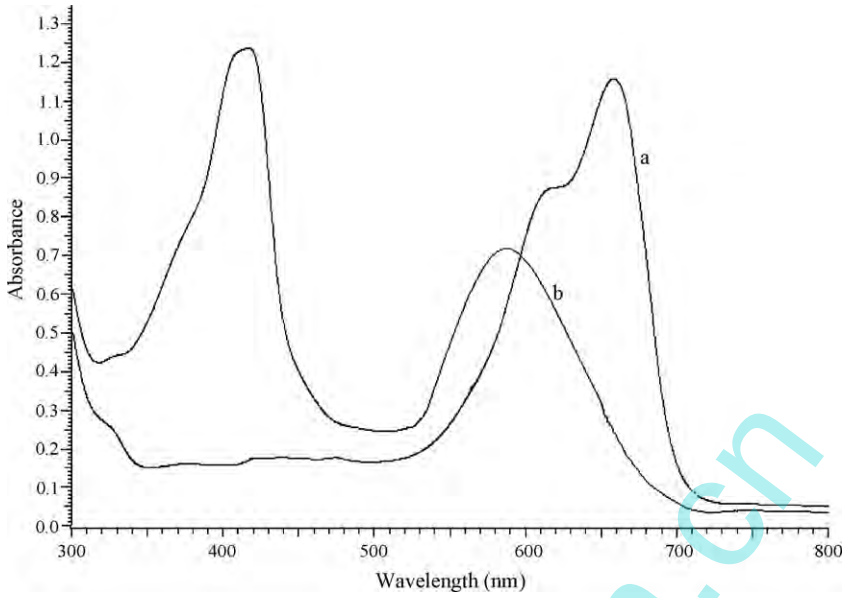

Fig. 2. UV–vis spectra of methylene green in solution (a) and in ormosil immobilized with HRP.

peak current was close to unity for MWCNTs modified electrode. It was clear that the peak potential was independent of the scan rate in the range between 10 and 200 mV s^{-1}. On the other hand, the MG/HRP/GCE shows poor electrochemical response for MG (Fig. 3a). As shown, the anodic and cathodic peaks were rather broad and the magnitude of the peak current was significantly lower than that observed on the MWCNTs composite electrode. Furthermore, the ΔE_p at the MG/HRP/GCE was relatively large, suggesting a sluggish electron transfer kinetics. From this result, we confirmed that MWCNTs/MG/HRP composites have good electrochemical reversibility. Both the anodic peak current and cathodic peak current were proportional to scan rate at the above scan range, suggesting that peak currents were surface confined. This suggested that redox dye as mediator was immobilized on the surface of the electrode successfully. The electrochemical behavior of MG modified with MWCNTs, without incorporated within ormosils was also investigated. MG molecules at once leached out from the electrode surface and no significant signal was observed (data not shown). To overcome this shortcomes, we used excellent ormosils matrix to encapsulate the MG and enzyme to increase the sensitivity and stability of hydrogen peroxide biosensor.

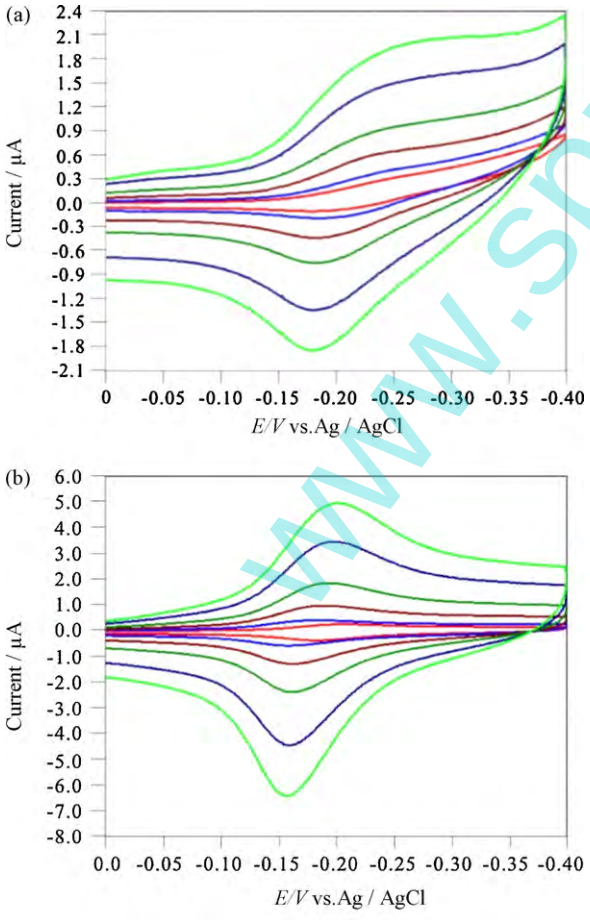

Fig. 3. Cyclic voltammograms of methylene green immobilized in ormosil in the absence (a) and presence (b) of MWCNTs in 0.1 M PBS (pH 7.2) at the scan rate of 5, 10, 20, 50, 100 and 200 mV s^{-1}.

Surface coverage (Γ) for the electroactive species was estimated by using Eq. (1)

$$\Gamma = \frac{Q}{nFA} \quad (1)$$

where A (0.70 cm^2) is the area of the working GCE, n (=1) the number of electron per reactant molecule, Q the charge obtained by integrating the anodic peak at low voltage scan rate (10 mV s^{-1}), and F is the Faraday Constant. In the present case, the calculated surface coverage for the electroactive species was 1.59×10^{-11} mol cm^{-2}.

3.3. Electrocatalysis of H_2O_2 on the MWCNTs/MG/HRP/GCE

At bare GC electrode, there was no response in the presence of H_2O_2. Fig. 4 displays the cyclic voltammograms of plane MG modified electrode without addition of H_2O_2 (curve A), and MG/HRP/GCE (curve B), MWCNTs/MG/HRP/GCE (curve C) in the presence of 0.5 mM H_2O_2 in 0.1 M PBS (pH 7.2) at the scan rate of 50 mV s^{-1}. It can been seen (Fig. 4, curve B) a small response was observed for MG/HRP/GCE in the potential range −0.05 to −0.18 V in the presence of 0.5 mM H_2O_2, but the modified electrode MWCNTs/MG/HRP/GCE (Fig. 4, curve C) showed a remarkable increased cathodic current in the same amount of H_2O_2. The reduction catalytic current of hydrogen peroxide starts at 0.0 V and obvious catalytic reduction peak appears at the potential of −0.18 V. This observation illustrated

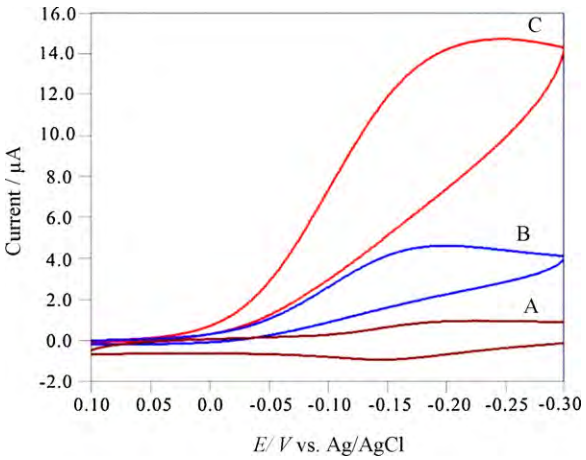

Fig. 4. Cyclic voltammograms of (A) plane MG incorporated in ormosil (B) and (C) are the CVs of MG/HRP/GCE and MWCNTs/MG/HRP/GCE respectively in the presence of 0.5 mM H_2O_2 in 0.1 M PBS (pH 7.2) at the scan rate of 50 mV s^{-1}.

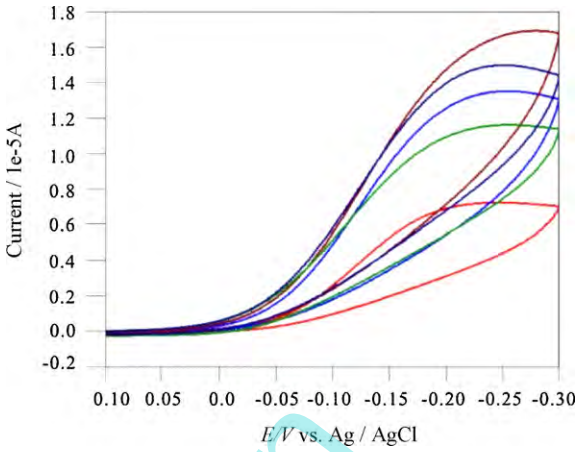

Fig. 5. Cyclic voltammograms of MWCNTs/MG/HRP/GCE in the presence of different concentration of H_2O_2: 0.3 0.5, 0.7, 1.0, 1.2 mM in 0.1 M PBS (pH 7.2) at the scan rate of 50 mV s^{-1}.

that MWCNTs played a significance role and facilitated the electrocatalysis of hydrogen peroxide on the modified electrode. MWCNTs not only increased the catalytic current, but also lowered the overpotential to reduce the interferences in the measurements. Fig. 5 presents the CVs of addition of various concentration of hydrogen peroxide at the scan rate of 50 mV s^{-1} in (0.1 M, pH 7.2) PBS. The cathodic peak current was dramatically increased and anodic peak current disappeared, indicated the fast electrocatalytic reduction of peroxide on the MWCNTs modified electrode.

The mechanism of the sensor can be summarized as follows. The peroxidase (POD) reduces hydrogen peroxide to water.

$$H_2O_2 + POD_{(red)} \rightarrow H_2O + POD_{(ox)}$$

Then the oxidized peroxidase converts MGH to MG^+

$$POD_{(ox)} + MGH \rightarrow POD_{(red)} + MG^+ + H^+$$

This overall reduction reaction of $POD_{(ox)}$ included two separate steps:

$$POD(I) + MGH \rightarrow POD(II) + MG^{\bullet}$$

$$POD(II) + MG^{\bullet} \rightarrow POD_{(red)} + MG^+$$

Where one electron was donated at a time, POD(I) was $POD_{(ox)}$ and $MG^{\bullet}$ represented the free radical formed during the reaction.

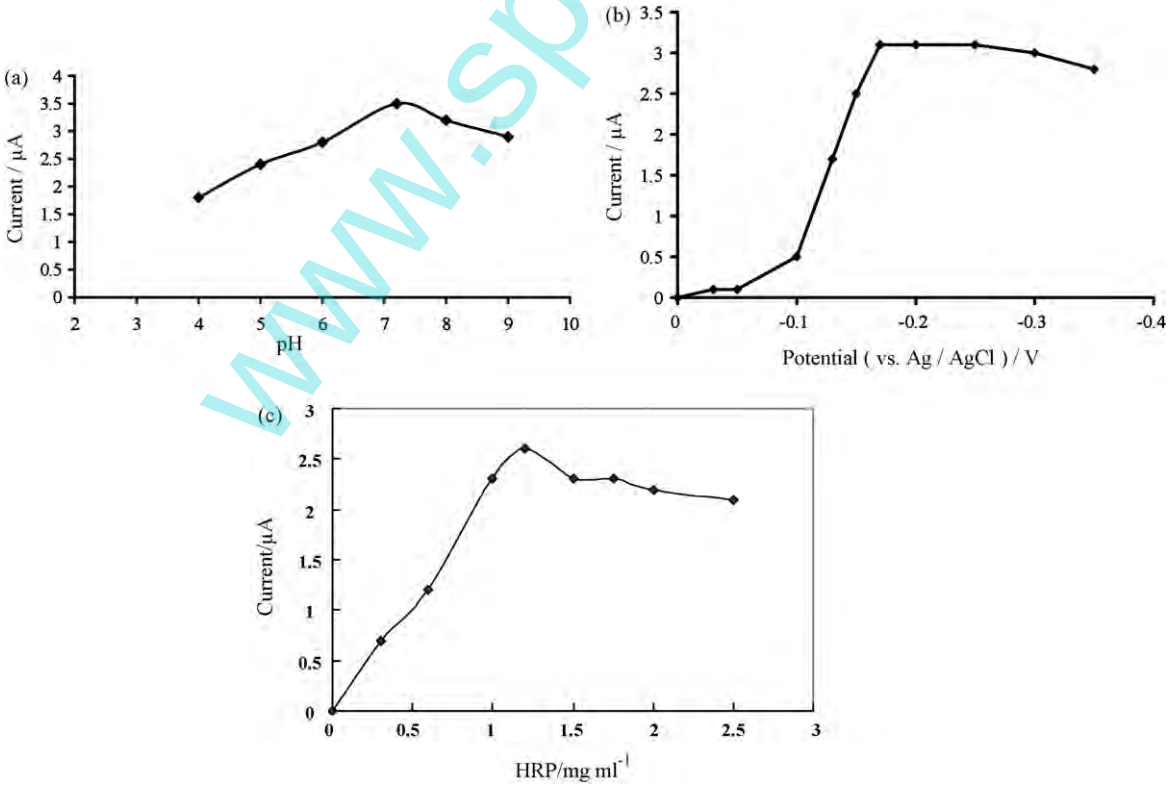

Fig. 6. (a) Influence of pH on the H_2O_2 sensor, study-state current measured in the presence of 0.5 mM H_2O_2 in 0.1 M PBS (pH 7.2) at applied potential of −0.18 at 25 °C. (b) Effect of potential on the sensor response for 0.5 mM H_2O_2 in 0.1 M PBS (pH 7.2). (c) Influence of the amount of HRP on the fabrication of biosensor.

MG^+ reduced at the sensor, resulting in a cathodic current.

$$MG^+ + H^+ + 2e \rightarrow MGH$$

3.4. Optimization of experimental conditions

3.4.1. Influence of pH and temperature on the sensor

It is well known that pH is a critical parameter of the enzyme activity and the stability in aqueous media [42]. The influence of the solution pH in the overall reaction for the electroanalysis of (0.5 mM) H_2O_2 using 0.1 M, PBS at pH 4.0 to 9.0 was studied Fig. 6a. The current and potential of the peak depended on the solution pH. The experimental results showed that the current response was higher at pH 7.2, when pH > 7.2/pH < 7.2, the current response became smaller. This was attributed to the higher activity of HRP in slight alkaline pH solution. Thus, the optimum pH for further studies was sit at 7.2.

The effect of temperature on the sensor had been examined between 15 and 45 °C. The response signal of the H_2O_2 sensor increased as the temperature varied from 15 to 37 °C. But at temperature lower than 20 °C, the activity of the enzyme was rather lower and the response time was relatively longer. On the other hand, at temperatures higher than 37 °C, the activity of enzyme decreased rapidly due to the partial denaturation of the enzyme. Taking both the lifetime and response time into consideration, 25 °C was the selected temperature for this work.

3.4.2. Effect of applied potential on the sensor

The applied potential has an important influence over the sensor response, because the applied potential contributes to the sensitivity and selectivity of the system [43]. The steady-state response to 0.5 mM H_2O_2 was measured at several applied potential values in 0.1 M, PBS buffer at pH 7.2, as shown in Fig. 6b. Electroreduction of H_2O_2 was observed already at approximately −0.18 V, and the steady-state current increased slowly with applied potential decreasing from −0.10 V to −0.18 V which can be attributed to the increasing driving force for the fast reduction of compounds. The current approaches a maximum value at −0.18 V and constant till −0.25 V, and then started decline. To avoid interferences and reduction of oxygen at high negative applied potential, −0.18 V was selected as the applied potential for amperometric measurement. This potential was superior to the previous reported work [44].

3.4.3. Influence of HRP amount on sensor fabrication

The amount of the enzyme in composite is a vital factor affecting the analytical sensitivity of the biosensor. The influence of amount of immobilized HRP on the analytical characteristics of the enzyme electrode was studied using CVs. Fig. 6c displays the effect of the amount of HRP enzyme in the MWCNTs modified electrode. The current response increases as the enzyme amount is increased and was maximum at 1.2 mg ml^{-1}. For higher amounts than 1.2 mg ml^{-1}, a reduction of the biosensor sensitivity is observed due to diffusion limitation. So, an optimum loading of 1.2 mg ml^{-1} HRP was used for subsequent experiment.

3.5. Kinetic analysis

The apparent Michaelis constant (K_M), which gives an indication of the enzyme-substrate kinetics, can be calculated from the electrochemical version of the Lineweaver–Burk equation

$$\frac{1}{I_{ss}} = \frac{1}{I_{max}} + \frac{K_M}{I_{max}}\frac{1}{C}$$

where I_{ss} is the steady-state current after the addition of substrate, C is the bulk concentration of the substrate and I_{max} is the maximum current measured under saturated substrate condition. The

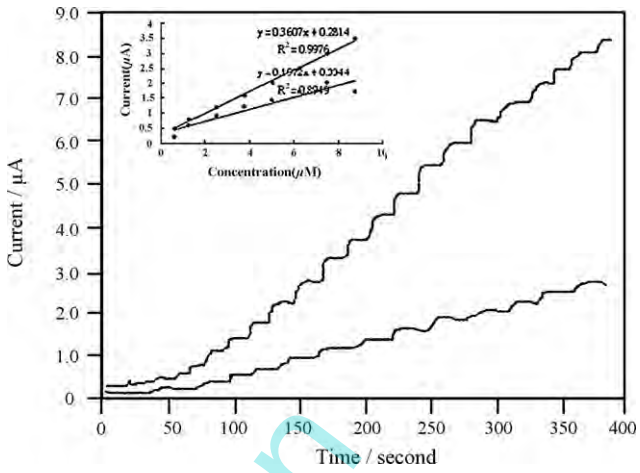

Fig. 7. Amperometric response of (a) MWCNTs/MG/HRP/GCE and (b) MG/HRP/GCE in a stirred 0.1 M PBS (pH 7.2) after successive hydrogen peroxide additions at applied potential −0.18 V vs. Ag/AgCl. Inset shows the linear calibration plot of catalytic currents vs. hydrogen peroxide concentrations.

K_M value was determined by analysis of the slope and intercept for the plot of the reciprocals of the cathodic current versus H_2O_2 concentration. The K_M value of the H_2O_2 sensor was determined by steady-state amperometric response and found to be 1.8 mM, which was smaller than those of 7.6 mM for HRP on nanoscopic gold tubes arrays modified nanoelectrode [45], 4.6 mM for HRP immobilized in sol–gel/hydrogel modified electrode [46], 4.3 mM for HRP in multilayer QPVP film [51], 4.51 mM for HRP on AuNP/CHIT/SPCE [47], 4.04 mM for HRP on TTF/TCNQ/MWCNTs modified electrode [30], 2.5 mM for HRP immobilized on a ferrocene containing polymer electrochemically deposited onto a Pt electrode [48], 5.12 mM for SBP (soybean peroxidase) immobilized in sol–gel thin film [49] and was close to 2.0 mM for HRP immobilized on FMC-BSA/MWCNTs ormosil composite-modified GC electrode [50] and 2.1 mM for sol–gel/nafion/MG electrode [32]. The smaller value of K_M value means that the immobilized HRP possesses higher enzyme activity, and the present modified electrodes exhibit higher affinity to H_2O_2. The immobilization of HRP in ormosils mentioned appears to be beneficial to improving the biosensor's performance.

4. Analytical characterization of H_2O_2 sensor

Fig. 7 presents the dynamic amperometric response of the sensor at a working potential of −0.18 V with successive injections of 0.5 mM H_2O_2 in 0.1 M PBS (pH 7.2) on MG/HRP/GCE and MWCNTs/MG/HRP/GCE. The trace clearly demonstrated the fast response and high sensitivity of the MWCNTs/MG/HRP/GCE to H_2O_2 than MG/HRP/GCE, suggested that the MWCNTs facilitated the electron transfer in the matrix and enhanced the electrocatalytic properties of modified electrode. The response time was less than 10 s (t = 95% of I_{max}), which was much lower than that earlier reported for H_2O_2 biosensor [52,53]. Fig. 6 (inset) shows the calibration plot of the biosensor. The response to H_2O_2 was linear in the range from 5×10^{-7} to 2×10^{-5} M with a correlation coefficient of 0.998 (n = 10), with the lower limit of detection 0.5 μM at a signal to noise ratio of 3. The higher sensitivity of the sensor may result from the biocompatible microenvironment around the enzyme [54]. The linear range, response time and limit of detection observed with MWCNTs/MG/HRP film electrode is in general comparable with most of the modified electrode reported in the literature (Table 2). The recovery rate was also estimated with the basic method of slandered recovery test. The recovery data were obtained as 98.6%.

Table 2
Comparison of the efficiency of MWCNTs/MG/HRP modified electrode used in determination of H_2O_2.

Electrode	Method	Electrolyte	LOD (μM)	LCR (M)	RT (s)	Ref.
MWCNT/MB/HRP/GCE	CV	pH 7 PBS	1	4×10^{-6} to 2×10^{-3}	<30	25
MWCNT/PS/HRP/SPE	CV	pH 7 PBS	25	2×10^{-5} to 5×10^{-4}	–	23
MWCNT/FMC-BSA/HRP/GCE	CV, FIA	pH 6.8 PBS	5	2×10^{-5} to 4.5×10^{-3}	20	24
PDDA-Au/DNA-Ag/HRP	CV	pH 6 PBS	2	7×10^{-6} to 7.8×10^{-3}	15	50
SG/MG/nafion/HRP/GCE	CV	pH 7 PBS	0.1	5×10^{-7} to 1.6×10^{-3}	20	32
MB/HRP/GA/GPE	CV	pH 7 PBS	3	9.9×10^{-6} to 6.49×10^{-4}	–	55
Ag-nano/PVA/Pt	CV	pH 7 PBS	10	45×10^{-6} to 6×10^{-3}	–	56
Gelatine/MB/HRP/GCE	CV	pH 7 PBS	4	1×10^{-5} to 1.2×10^{-3}	<20	40
NMB/HRP/GCE	CV	pH 7 PBS	2.07	2.5×10^{-6} to 1×10^{-4}	<20	57
MG/HRP/zeolite/GCE	CV	pH 7 PBS	0.5	2.5×10^{-6} to 2.4×10^{-4}	40	44
MWCNT/MG/HRP/GCE	CV	pH 7.2 PBS	0.5	5×10^{-7} to 2×10^{-5}	<10	Present work
PEGDGE/SBP/GCE	CV	pH 7.4 PBS	–	1×10^{-7} to 2×10^{-4}	–	58

LCR: linear concentration range; LOD: limit of detection; RT: response time.

Table 3
Interferences studies.

Interferents	Current ratio
Uric acid	1.01
Glucose	1.00
Cysteine	1.00
Dopamine	1.03
Ascorbic acid	1.00
Oxalic acid	0.97
NADH	1.00
Citric acid	0.99

4.1. Stability of the biosensor

The stability of the biosensor was examined by amperometric measurements in the presence of 6 μM H_2O_2 periodically. It was found that the biosensor retained its 90% response after 1 month of testing. When the biosensor was not in use, it was stored under dry conditions at 4 °C in a refrigerator. The good long-term stability can be attributed to the great stability of MG and the excellent biocompatibility and the stabilizing microenvironment around the HRP provided by the organically modified sol–gel composite matrix.

4.2. Selectivity against interferences

The selectivity of this H_2O_2 biosensor was evaluated by H_2O_2 determinations in the presence of some potentially coexisting compounds of H_2O_2 in biological systems. In this experiment, six interfering substances including uric acid, dopamine, ascorbic acid, glucose, cysteine, oxalic acid, NADH and citric acid were tested and the results were listed in Table 3. It can be observed that the eight tested interferents exerted neglectable influences on the determination of H_2O_2.

5. Conclusion

We have developed a novel MWCNTs/ormosils based electrochemical biosensor for the analytical detection of hydrogen peroxide. HRP and MG were successfully incorporated within ormosils matrix. The experimental results proved that the MWCNTs imparting the electrocatalytic property of modified electrode due to enhance the rate of electron transportation within omosils film. The modified electrode MWCNTs/MG/HRP/GCE showed stable and reproducible electrochemical behavior, long stability and excellent electrochemical reversibility. This modified electrode showed excellent electrocatalytic activity for H_2O_2 reduction at reduced over potential with fast response time (<10 s) with very low limit of detection. So, this novel and efficient strategy, that is, successful coimmobilization of HRP, MG as a mediator, and MWCNTs within ormosils for the construction of the hydrogen peroxide biosensor, opens up a new approach to construct verity of organically modified sol–gel glasses amperometric biosensors.

Acknowledgement

This work was financially supported by the National Science Council of Taiwan.

References

[1] S.Q. Liu, H.X. Ju, Biosens. Bioelectron. 19 (2003) 177.
[2] X.B. Lu, J.H. Jhou, W. Lu, Q. Liu, J.H. Li, Biosens. Bioelectron. 23 (2008) 1236.
[3] X.H. Shu, Y. Chen, H.Y. Yuan, S.F. Gao, D. Xiao, Anal. Chem. 79 (2007) 3695.
[4] X. Cui, G. Liu, Y. Lin, J. Biomed. Nanotechol. 1 (2005) 1.
[5] X.L. Luo, J.J. Xu, W. Zhou, H.Y. Chen, Biosens. Bioelectron. 19 (2004) 1295.
[6] M.C.Y. Chang, A. Pralle, E.Y. Isacoff, C.J. Chang, J. Am. Chem. Soc. 126 (2004) 15392.
[7] J. Li, P.K. Dasgupta, G.A. Tarver, Anal. Chem. 75 (2003) 1203.
[8] N.V. Klassen, D. Marchington, H.C.E. McGovan, Anal. Chem. 66 (1994) 2921.
[9] A. Lobnik, M. Cajlakovuc, Sens. Actuators B 74 (2001) 194.
[10] S.H. Chen, R. Yuan, L.Y. Zhang, N. Wang, X.L. Li, Biosens. Bioelectron. 22 (2007) 1268.
[11] J. Li, C. Lau, M. Morizono, K. Ohta, M. Kai, Anal. Chem. 73 (2001) 5979.
[12] A.A. Karyakin, Electroanal. 13 (2001) 813.
[13] J. Wang, M. Gu, J. Di, Y. Gao, Y. Wu, Y. Tu, Biopro. Biosyst. Eng. 30 (2007) 289.
[14] W. Li, R. Yuan, Y. Chai, L. Zhou, S. Chen, Na Li, J. Biochem. Biophys. Methods 70 (2008) 830.
[15] V. Lvovich, A. Scheeline, Anal. Chem. 69 (1997) 454.
[16] S. Iijima, Nature 354 (1991) 56.
[17] L.Q. Rong, C.Y.Q.Y. Qian, X.H. Xia, Talanta 72 (2007) 819.
[18] N. Zhu, Z. Chang, P. He, Y. Fang, Anal. Chim. Acta 545 (2005) 21.
[19] K. Gong, Y. Dong, S. Xiong, Y. Chen, L. Mao, Biosens. Bioelectron. 20 (2004) 253.
[20] J. Manso, M.L. Mena, P. Yanez-Sedeno, J. Pingarron, J. Electroanal. Chem. 603 (2007) 1.
[21] A. Salimi, L. Miranzadeh, R. Hallaj, H. Mamkhezri, Electroanalysis 20 (2008) 1760.
[22] Y. Liu, J. Lei, H. Ju, Talanta 74 (2008) 965.
[23] S. Sanchez, M. Pumera, E. Cabruja, E. Fŕbregas, Analyst 132 (2007) 142.
[24] V.S. Tripathi, V.B. Kandimalla, H. Ju, Biosen. Bioelectron. 21 (2006) 1529.
[25] Jin. Xu, J. Zhu, Q. Wu, Z. Hu, H. Chen, Electroanalysis 15 (2003) 219.
[26] B. Wang, J.J. Zhang, Z.Y. Pan, X. Tao, H. Wang, Biosen. Bioelectron. 24 (2009) 1141.
[27] Po.H. Lo, S.A. Kumar, S.M. Chen, Colloid Surf. B: Biointerfaces 66 (2008) 266.
[28] A.K.M. Kafi, G. Wu, A. Chen, Biosen. Bioelectron. 24 (2008) 566.
[29] J.L. Lyon, K.J. Stevenson, Electron. Chim. Acta 53 (2008) 6714.
[30] Z. Cao, X. Jiang, Q. Xie, S. Yao, Biosen. Bioelectron. 24 (2008) 222.
[31] J. Liu, S.L. Mu, Synth. Met. 107 (1999) 159.
[32] B. Wang, S. Dong, Talanta 51 (2000) 565.
[33] A. Vasilescu, S. Andreescu, C. Bala, S.C. Litescu, T. Naguer, J.L. Martr, Biosens. Bioelectron. 18 (2003) 781.
[34] A. Noorbakhsh, A. Salimi, E. Sharifi, Electroanalysis 20 (2008) 1788.
[35] R. Gupta, N.K. Chaudhury, Biosen. Bioelectron. 22 (2007) 2387.
[36] T. Coradin, J. Livage, Acc. Chem. Res. 40 (2007) 819.
[37] D. Avnir, O. Lev, J. Livage, J. Mater. Chem. 16 (2006) 1013.
[38] S. Xu, Z. Jiang, H. Wu, S. Huang, Progr. Chem. 16 (2004) 443.
[39] A.F. Groboilot, C.P. Champagne, G.D. Darling, D. Poncelet, R.J. Neufild, Biotechnol. Bioeng. 42 (1993) 1157.
[40] H. Yao, N. Li, S. Xu, Jin. Xu, J.J. Zhu, H. Chen, Biosen. Bioelectron. 21 (2005) 372.
[41] S. Jockusch, N.J. Turro, Macromolecules 28 (1995) 7416.
[42] G. Bicketstaff, Methods in Biotech, Humana Press, New Jersey, 1997.
[43] E. Csoregi, G. Jonsson-Petersson, L. Gorton, J. Biotechnol. 30 (1993) 315.
[44] B. Liu, F. Yan, J. Kong, J. Deng, Anal. Chim. Acta 386 (1999) 31.

[45] M. Delvaux, A. Walcarius, S. Demoustier-Champagne, Anal. Chim. Acta 525 (2004) 221.
[46] B. Wang, J. Zhang, G. Cheng, S. Dong, Anal. Chim. Acta 407 (2000) 111.
[47] T. Tangkuaram, C. Ponchio, T. Kangkasomboon, P. Katikawong, W. Veerasai, Biosen. Bioelectron. 22 (2007) 2071.
[48] M.P.G. Armada, J. Losada, I. Cuadrado, B. Alonso, B. González, C.M. Casado, J. Zhang, Sens. Actuators B 101 (2004) 143.
[49] Q. Wang, G. Lu, B. Yang, Anal. Chem. 71 (1999) 1935.
[50] L. Ma, R. Yuan, Y. Chai, S. Chen, J. Mol. Catal. B 56 (2009) 215.
[51] C. Sun, W. Li, Y. Sun, X. Zhang, J. Shen, Electrochim. Acta 44 (1999) 3401.
[52] H. Liu, Y. Liu, J. Qian, T. Yu, J. Deng, Talanta 43 (1998) 111.
[53] C. Lei, J. Deng, Ana. Chem. 68 (1996) 3344.
[54] B.Q. Wang, B. Li, Q. Deng, S.J. Dong, Anal. Chem. 70 (1998) 170.